The PHENIX Lead-Scintillator Electromagnetic Calorimeter: Test Beam and Construction Experience [1]

G.David, Y.Goto[2], E.Kistenev, S.Stoll, S.White, C.Woody
Brookhaven National Laboratory, Upton, New York

A.Bazilevsky, S.Belikov, S.Chernichenkov, A.Denisov, V.Kochetkov, Y.Melnikov, V.Onuchin, V.Semenov, V.Shelikhov, A.Soldatov, A.Usachev Institute for High Energy Physics, Protvino, Russia

Abstract

We have recently completed the production of the 15552 channel Lead-Scintillator Electromagnetic calorimeter for the PHENIX experiment at RHIC. Our design features a single 4 tower module which is repeated throughout and which was produced with a number of quality control steps designed to achieve consistent, large light yields in all channels. We present results on the uniformity of the calorimeter, accuracy of a cosmic muon based precalibration scheme and test beam performance.

I. INTRODUCTION

The Physics of heavy ion collisions has as a major goal the detection of the Quark-Gluon Plasma. The PHENIX experiment at RHIC [1] is optimized for the detection of electromagnetic probes (e, γ, μ) of this new form of matter and the electromagnetic calorimeter plays a decisive role in these measurements. The calorimeter is used to measure electron and photon production in relativistic heavy ion collisions at RHIC, and will be an integral part of the particle identification and trigger system for PHENIX. In addition, the calorimeter will be used to measure high p_T photon production and other electromagnetic processes in high energy polarized proton collisions as part of the spin physics program at RHIC.

The EMCal covers the rapidity range +-0.35 units and an azimuthal angle of 180 degrees. It is subdivided into 8 equal coverage sectors. Six sectors are lead-scintillator (PbSc) sampling calorimeters custom developed and built for PHENIX in Russia [2], [3] , and the rest is covered by two lead glass Cherenkov Sectors imported from the WA98 experiment at CERN.

The PbSc electromagnetic calorimeter is a shashlik type detector consisting of 15552 individual towers and covers an area of approximately 48 m^2. The calorimeter has a nominal energy resolution of $8\%/\sqrt{E(GeV)}$ and a timing resolution of $\leq$ 100 ps for electromagnetic showers [2]. An extensive precision calibration and monitoring system has been developed to achieve a predetermined absolute energy calibration of less than 5% for day one operation at RHIC, and to maintain an overall long term gain stability of better than 1%.

II. DESIGN AND PRODUCTION PERFORMANCE

The PbSc EMCal is built of optically independent readout towers containing 66 sampling cells, 1.5mm of Pb and 4mm of injection molded Sc, ganged together by penetrating wavelength shifting fibers for light collection. An important feature of this light collection technique is that it gives a large photon yield and good uniformity. The short distance the light travels to the WLS fibers eases the requirements on the light attenuation in the scintillator and allows the consideration of alternative scintillator production technologies. Four towers are mechanically grouped together into a single entity called a Module, as shown in Fig. 1.

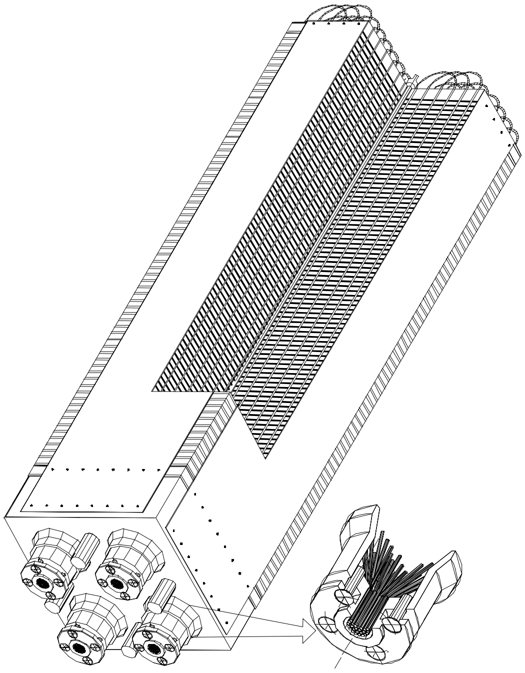

Fig. 1 Interior view of calorimeter module showing stack of scintillator and lead plates, wavelength shifting fiber readout, and leaky fiber inserted in central hole

Thirty six modules are attached to a backbone and held together by welded stainless steel skins on the outside to form a rigid supermodule. The purpose behind this grouping is to create a building block with a minimum of supporting

[1]This work was supported under DOE Contract DE-AC02-76CH00016

[1]Visitor from RIKEN (The Institute for Physical and Chemical Research), Wako, Saitama, Japan

components which can be easily assembled on a production line.

A short summary of the major EMCal design parameters is given in Table 1

Table 1
Lead-Scintillator Calorimeter Parameters

Item	Parameters
Lateral segmentation	$5.25 \times 5.25\ cm^2$
Active cells	66
Scintillator	4 mm, Polystyrene based 1.5% PT / 0.01% POPOP
Absorber	Pb, 1.5 mm
Cell thickness	5.6 mm (0.277 $X_\circ$)
Active depth	375 mm
WLS fibers per tower	36
Fiber	BCF-99-29a, 1 mm
PMT type	FEU115M, 30 mm MELS, Russia
Photocathode	Sb-K-Na-Cs
Luminous sensitivity	$\geq$ 80 μa/lm
Rise time (20%–80%)	$\leq$ 5 ns

During production we screened for both mechanical tolerances and light yield of scintillators with a weak radioactive source (about 2% of all tiles). Final acceptance tests made on every module included excitation of the individual tiles in every assembled tower by UV light from a laser and measuring the tower response with well calibrated photomultipliers. Consistency of the whole procedure was verified by comparing relative variations in the light yield measured at the production site to those seen exposing the towers to cosmic muons, as shown in Fig. 2.

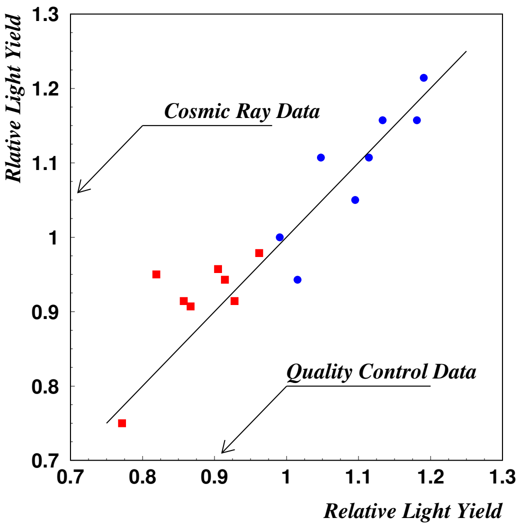

Fig. 2 Correlations between EMCal tower response to laterally penetrating μ's and laser excitation

To emphasize the point, the figure combines the data for modules built using fibers of different quality, thus artificially increasing the observed spread in the light yield among the modules.

The calorimeter is designed with the phototubes installed very close to the last scintillating tile. Consequently, the light exiting the fibers is comprised of two distinct components characterized by different attenuation lengths (core & cladding light). Typical attenuation curves measured scanning an assembled calorimeter tower with a radioactive source and with cosmic μ's is shown in Fig. 3. The effective attenuation

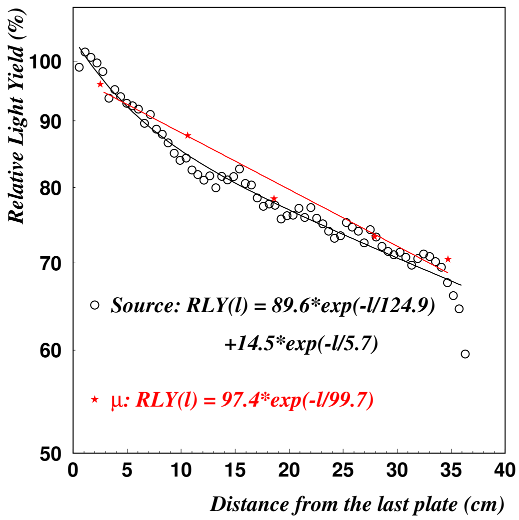

Fig. 3 Light attenuation in a PbSc EMCal module

curve resulting from the two components being superimposed agrees well with a single exponential parametrization with an attenuation length of ∼120 cm, and only a small admixture of a component with a shorter attenuation length.

The calibration and monitoring system is based on a UV laser which supplies light to the calorimeter through a system of optical splitters and fibers. The block diagram of the monitoring system is shown schematically in Fig. 4 [4].

Light from a high power YAG laser is initially split into six equal intensity beams using a set of partially reflecting mirrors. The beam from each mirror passes through a quartz lens and is focused to a point just in front of a quartz fiber which is used to transport the light over a distance of approximately 50 meters to each sector of the calorimeter.

A system of optical splitters is used to distribute the light to each of the individual calorimeter modules. The light is injected into a 38 cm long × 2 mm dia. plastic "leaky fiber" which allows the light to leak out of the fiber in such a way as to simulate a 1 GeV electromagnetic shower penetrating along the depth of the module. The overall efficiency to convert the primary light from the laser to photoelectrons in an individual module is of order 4×10^{-12}. Given that the calorimeter has an intrinsic light output of $\sim$ 1500 photoelectrons per GeV, this leads to an energy requirement of $\sim$ 0.2 mJ per pulse from the YAG laser to deliver 1 GeV of equivalent energy to each tower.

Under normal conditions the EMCal monitoring system system permits following the system gain variations to better

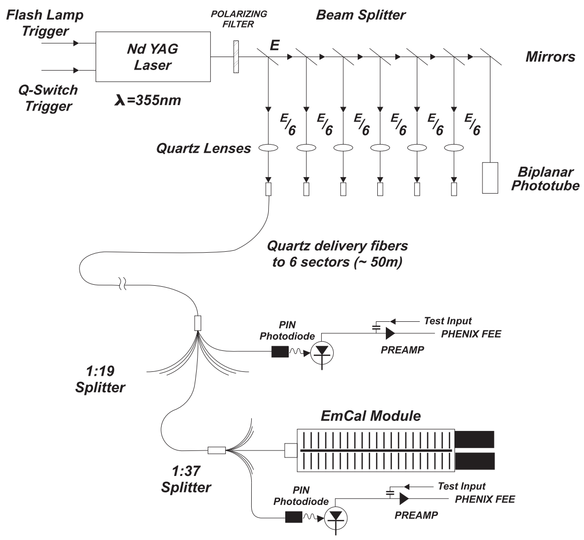

Fig. 4 Laser light distribution and monitoring system

then 1%. If a phototube is replaced, variations in the system gain could reach few %. The latter limitation is due to the leaky fiber being effectively coupled to very few wave-length shifting fibers near the corner of the scintillting tiles.

Construction of the calorimeter is now nearing completion. A precalibration scheme was developed which is based upon simultaneously recording the calorimeter response to cosmic μ's penetrating the supermodule in the direction nearly orthogonal to the tower axis and the response due to laser exitation. A lego plot of the energies deposited by a penetrating μ inside the supermodule towers is shown in the bottom left corner of Fig. 5.

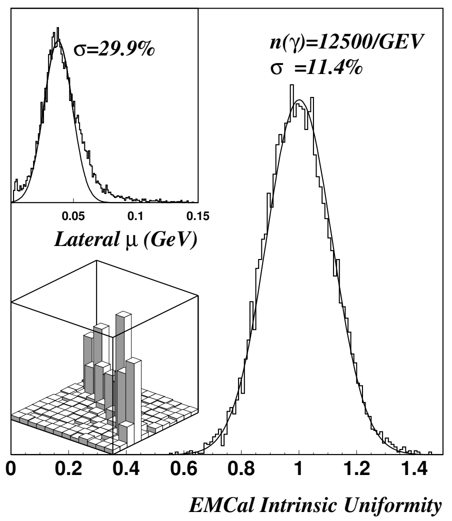

Fig. 5 Uniformity of the Light Yield in the PHENIX EMCal. Inserts: (top) - Energy distribution in the EMCal tower exposed to laterally penetrating cosmic μ's; (bottom) - Lego plot of energies deposited in the EMCal towers by laterally penetrating cosmic μ.

The top left corner in the same figure is the energy spectrum in one tower exposed to laterally penetrating μ's. It peaks at 38 MeV and has a nearly gaussian shape with $\sigma(E)/E$ ~30%. On average the EMCal towers produce 12500 γ's per 1 GeV of deposited electromagnetic energy. The distribution of the light yield (normalized to an average value) for ~8000 towers is also shown in Fig. 5. The original light yield measurements are performed with a "standard set" of phototubes, whose quantum efficiences (QE) and gains differ from the actual tubes used in the final assembly. We use the laser light amplitude to correct for QE and gain differences.

The calorimeter will run with a common high voltage applied to groups of 48 photomultiplies. While randomly chosen PMT's may have factor of 10 difference in their gains at the same voltage, the triple product *System Gain = Light Yield × PMT Gain × PMT Quantum Efficiency* is expected to differ by no more then 5% over the whole EMCal. This matching is done primarily to achieve uniform triggering conditions, with the goal of equalizing the system gains to better than 10%. To achieve this goal, gain curves for all PMT's are measured and stored in a data base. The data base is then independently scanned for every group of 48 counters in an attempt to find the match satisfying the trigger requirements. However, the final gain tuning will be made using a Variable Gain Amplifiers built into our readout chain.

The distribution of laser amplitudes (normalized to the average value) for the gain-balanced calorimeter is shown in Fig. 6. The data for different supermodules were combined together assuming that the amount of the light delivered to individual supermodules was tuned to compensate for the differences in the average efficiencies of the 1:37 splitters (see Fig. 4). The predicted intrinsic nonuniformity of the light delivery system is below 13% . While it is not necessary to have a uniform system response to monitoring laser pulses, reaching this goal will help to minimize the amount of time data for monitoring purposes.

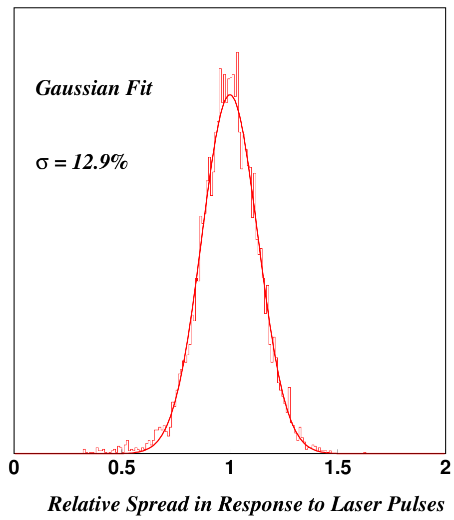

Fig. 6 Uniformity of the EMCal response to Laser pulses. Dashed distribution is for the uniform 1:19 light split (see Fig. 4), top histogram and a Gaussian fit are for the optimized 1:19 split.

III. Test Beam Performance

A. Energy and position measurements

Pions up to $\sim 0.3\ GeV/c$ and protons up to $\sim 0.9\ GeV/c$ are totally absorbed in the calorimeter. The line shapes measured in the calorimeter for $1\ GeV/c$ π's, protons and electrons are shown in Fig. 7.

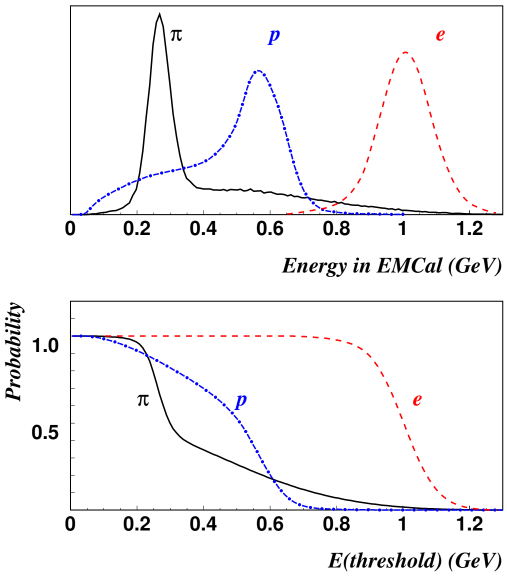

Fig. 7 Top: EMCal response to 1 GeV/c π's, p's and electrons. Bottom: The probability for 1 GeV/c π's, p's and electrons to deposit energy in the EMCal above $E(threshold)$

Hadronic line shapes are nongaussian, with π's exhibiting a characteristic minimum ionizing peak at $270\ MeV$ and a long tail extending towards the total available energy. Protons at $1\ GeV/c$ nearly range out in the calorimeter and produce a straight through peak at $\sim\ 566\ MeV$. Both values are in agreement with the sampling fraction values as predicted from GEANT $\epsilon(e) : \epsilon(\pi) : \epsilon(p) = 0.19 : 0.27 : 0.31$. The 8% width of the energy distribution for electrons at 1 GeV agrees very well with our previously measured [2] energy resolution of:

$$\sigma(E)/E = 1.5 \oplus 8.0/\sqrt{E(GeV)},$$

and pion rejection factor $\sim\ 100$ for pion momenta above 2 GeV/c.

A detailed GEANT simulation shows that in Au+Au events with a characteristic multiplicity of a few hundred particles per unit rapidity, the calorimeter will on average measure 60% of the energy within its aperture with a resolution depending on the aperture. A value of $\sigma \sim 10\%$ was computed for a coverage corresponding to a single EMCal sector($2 \times 4\ m^2$ at 5 m from the collision point) in central Au+Au collisions.

Our earlier measurements of the EMCal position resolution were published elsewhere[2]. New measurements were made to improve the understanding of calorimeter response to particles over a wide angular range.

Figure 8 combines the simulated GEANT shower shapes for three angles of incidence and GEANT predictions for the position resolution as function of the angle of incidence in the energy range $0.5 \div 8.0\ GeV/c$ and the experimental points measured in the test beam at the AGS.

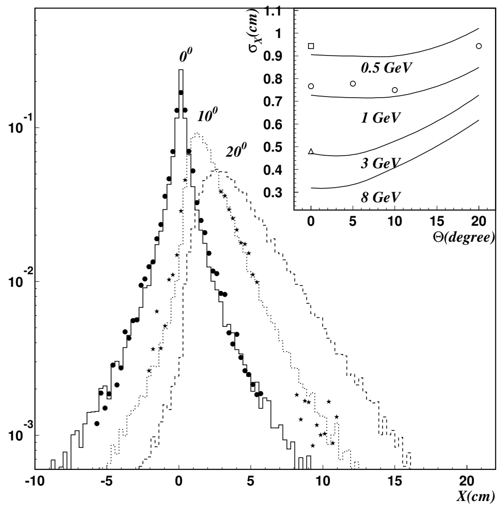

Fig. 8 Projected shower shape in EMCal exposed to 1 GeV/c electrons for different angles of incidence. Insert: EMCal position resolution.

Both GEANT and the experimental data show that the shower projection onto the calorimeter front face becomes skewed at nonorthogonal angles of incidence. The data also show a gradual dilution of the shower core, mainly related to the longitudinal shower fluctuations contributing to the width of the projected shower. We used the shower centroid as a zero approximation for the impact position and a combination of experimental data and GEANT simulation to parameterize the systematic effects related to the discrete nature of the calorimeter measurements, and to the modifications to the projected shower shape for nonorthogonal impacts:

$$X_{cg} \ = f(X_{imp},\, \theta) \ = \frac{sh(\phi)}{2 \times sh(\frac{1}{2b(\theta)})} + \Delta,$$

where

θ = impact angle measured with respect to normal incidence,

$$\phi = \frac{X_{impact}}{b(\theta)} - \phi_0(\theta),$$

Δ = shower median x sin(θ),
$b(\theta)$ = shower width

and $\phi_0(\theta)$ is the phase shift related to the skewed shape of shower projection.

We found that the shower width depends on impact angle as

$$b(\theta) \ = b_0 + a(E) * sin^2(\theta),$$

Table 2

π^0 mass measurements in EMCal

Beam Momentum (GeV/c)	3	5	5	7
Distance from Target (cm)	169	169	239	239
Test Beam Data				
Fitted π^0 mass (MeV)	133.1	134.1	137.1	135.6
	$\pm$0.8	$\pm$0.5	$\pm$1.0	$\pm$0.4
σ of the fit (MeV)	15.0	16.3	12.1	14.6
	$\pm$0.7	$\pm$0.5	$\pm$0.9	$\pm$0.4
GEANT predictions				
Fitted π^0 mass (MeV)	134.9	135.3	135.2	134.8
σ of the fit (MeV)	13.2	15.8	11.5	13.8
σ(X) Contr. (MeV)	9.0	13.5	8.6	12.1
σ(E) Contr. (MeV)	8.0	7.2	6.5	6.4

where b_0 = 7.8 mm is an energy independent electromagnetic shower width for $\theta = 0$. The increased shower width for nonorthogonal angles of incidence results in improved position resolution for small angles (see insert). At a larger angles, the contribution from longitudinal fluctuations becomes dominant and the position resolution degrades. All available data on position resolution can be well described by the simple formula

$$\sigma(X) \ = \sigma_0(E) \oplus \Delta * sin(\theta),$$

where

$$\sigma_0(E) = 1.55 + \frac{5.7}{\sqrt{E}} \ (mm), \qquad E(GeV)$$

is the position resolution for normal incidence and $\Delta \ \sim \ L_{rad}$.

B. *Effective mass measurements*

A critical test of the calorimeter performance is its ability to measure multiphoton effective masses with predictable resolution. This issue was addressed by exposing one of the production calorimeter supermodules initially calibrated with cosmic μ's to neutral particles produced from interactions of π^- mesons in a plexiglass target upsteam of the calorimeter. Veto counters downstream of the target provided an efficient neutral trigger, and a standard EMCal pattern recognition program was used to identify individual showers, and to compute energies and positions of the impinging particles . A typical 2γ effective mass distribution observed in a 7 GeV/c exposure is shown in Fig. 9. A summary of the π^0 mass measurements, together with the results of a GEANT simulation, is given in Table 2.

The data also show the presence of the η meson, but with much lower statistics. The η mass measured in the 7 GeV/c exposure is equal to 0.548 $\pm$0.005 MeV, and the distribution has a fitted width of 33$\pm$4 MeV, compared to a 27 MeV width predicted by the GEANT simulation.

All beam data agree with the simulation within one standard deviation, and confirms that uncertainties related to the smooth approximation of the pattern of nonuniformities

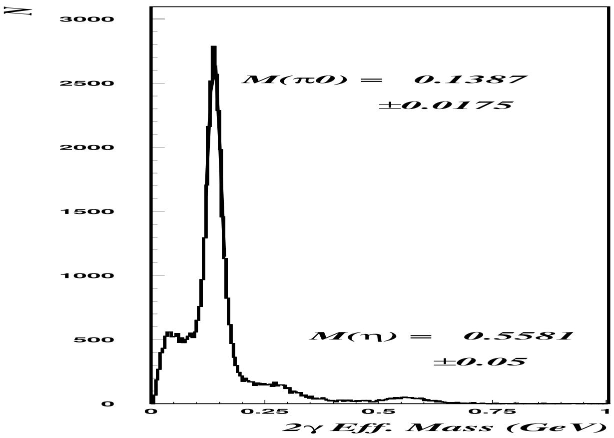

Fig. 9 Two-photon effective mass distribution measured exposing single EMCal supermodule in the beam of negative π's. Target $\sim 3\ m$ upstream of the calorimeter.

in the calorimeter (local hot spots around fibers etc) and the contribution of electronics noise, are small compared to the effects of cell size, sampling and shower fluctuations.

IV. Time of Flight Measurements with Calorimeter

The interest in the timing resolution of the calorimeter is stimulated by the idea of using the timing information as a particle identification tool, for pattern recognition, and to reject background hits. The timing response of the PbSc calorimeter was studied extensively exposing the calorimeter to electron and hadron beams in the momentum range 0.3 - 5 GeV/c [2]. The major obstacles to using the calorimeter for ToF measurements were large range of amplitudes and variations in the pulse shape depending upon the nature and energy of the particle.

The differences in the light and shower propagation speeds in the calorimeter result in the PMT seeing the light from the last tile nearly 1.5 ns earlier than from the first tile. Combined with the particle and energy-dependent showering characteristics, this results in systematic differences between the arrival times of electrons and hadrons. Figure 10 summarizes the data on systematic differences between arrival times for μ's, π's and p's at three different momenta. The picture shows the energy distributions in the timing tower (top) and the dependence of the arrival time (measured with respect to electrons depositing similar energy in the tower) on the energy in the tower. Towers with low deposited energies (periphery of the showers) see hadrons delayed with respect to electrons. However penetrating particles and fully developed hadronic showers produce a timing signal $\sim 200ps$ earlier than electrons.

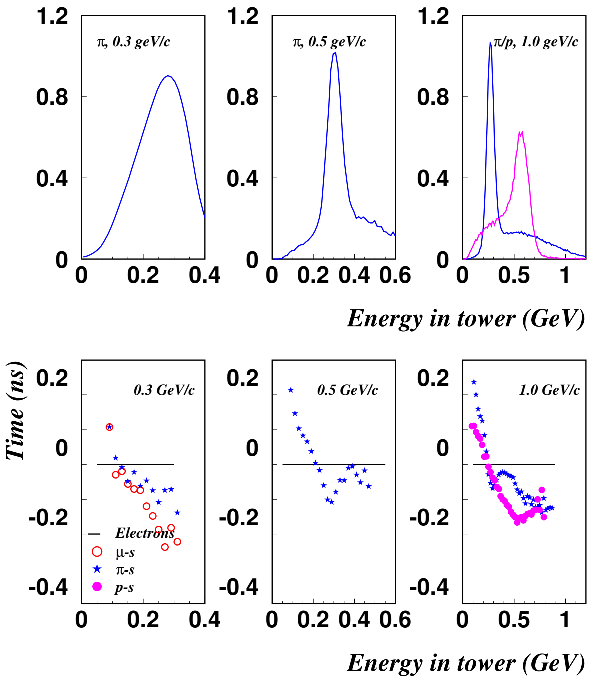

Fig. 10 Particle type and particle momentum dependence of the systematic in the EMCal ToF measurements

Walk corrected arrival times measured by exposing the calorimeter to electrons, π's and p's at 1 GeV/c momenta are shown in the top of Fig. 11. The distribution for electrons has a perfectly gaussian shape with only a few events in the tails. Both the π and p distributions show the presence of tails (as one would expect from Fig. 10) and are slightly asymmetric.

The timing resolution curves (stochastic term) plotted in Fig. 11 combine the points measured by exposing the calorimeter to particles in the 0.3 - 1 GeV/c momentum range.

The timing resolution for very low deposited energies is driven by the proximity of the maximum signal amplitude to the threshold on the timing discriminator. Above the discriminator threshold, the calorimeter timing resolution is nearly constant ($\sim 100ps$ for electrons, $\sim 200ps$ for hadrons) due to the fact that shower fluctuations are the major contributor to the measured rms values. In general, the data can be well fitted by the function:

$$\Delta t = \Delta t_0 + \Delta t_1/(E - E_{threshold}), \qquad E\ GeV/c,$$

which includes a pole type divergence close to threshold. Here Δt_0 is an intrinsic timing resolution limit, presumably due to fluctuations in the localization of the shower, and Δt_1 includes contributions due to photon statistics and pulse shape fluctuations. The latter is dominant close to threshold, and may be tuned by adjusting the gain of the phototubes and discriminator thresholds.

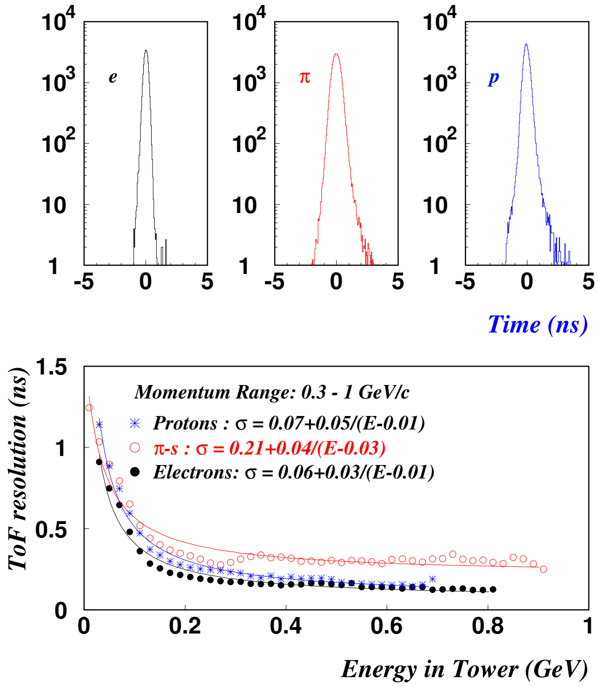

Fig. 11 EMCal timing resolution for different particles in the momentum range 0.3÷ 1 GeV/c

V. Summary

We designed and successfully constructed a 15 552 channel electromagnetic calorimeter covering total area of 48 m^2 for the PHENIX experiment at RHIC. The design was optimized for industrialized mass production which relied heavily on industrial style quality control procedures to insure conformity to the physics specifications.
The calorimeter energy and position resolution ($\sim$8% and $\sim$7 mm respectively for 1 GeV photons and electrons at a normal incidence) is sufficient to measure the π^0 mass with resolution $\sim$15 MeV.
The EMCal has an excellent timing resolution ($\sim$100 ps for electromagnetic and $\sim$200 ps for hadronic activities) which is nearly independent of the energy. Systematics in the calorimeter timing measurements was studied in great detail and understood. We believe that in addition to providing PHENIX with a measure of photon and electron probes of the QGP, its excellent timing performance will greatly enhance thecapability of PHENIX for studying the QGP via hadronic probes.

VI. References

[1] PHENIX Conceptual Design Report, BNL 48922, January 29, 1993

[2] E.Kistenev et.al.,"PHENIX PbSc Electromagnetic Calorimeter: Results of Test Beam Studies", *Proceedings of the Fifth International Conference on Calorimetry in High Energy Physics* World Scientific (1994) 211-223.

[3] G.David et.al.,"Performance of the PHENIX EM Calorimeter", *IEEE Trans. Nucl. Sci.* Vol.43, No.3, June 1996

[4] G.David et.al.,"The Calibration and Monitoring System for the

PHENIX Lead-Scintillator Electromagnetic Calorimeter", *IEEE Trans. Nucl. Sci.* (1997) submitted for publication.